

# Simulation of hydro-formability testing for tubes

A.H. van den Boogaard<sup>1</sup>, M.H. Kelder<sup>2</sup>

<sup>1</sup>*Faculty of Engineering Technology, University of Twente, P.O. Box 217, 7500 AE Enschede, Netherlands  
URL: [www.tm.ctw.utwente.nl](http://www.tm.ctw.utwente.nl)  
e-mail: [a.h.vandenboogaard@ctw.utwente.nl](mailto:a.h.vandenboogaard@ctw.utwente.nl)*

<sup>2</sup>*Corus RD&T, P.O. Box 10000, 1970 CA IJmuiden, Netherlands  
e-mail: [maarten.kelder@corusgroup.com](mailto:maarten.kelder@corusgroup.com)*

**ABSTRACT:** With the development of dedicated tubular products for hydroforming, the need for a representative test for these products evolves. Currently free expansion tests are used, but these tests only follow a more or less plane strain deformation. In reality, hydroforming is used with end feeding and the plane strain deformation is not representative. By performing a number of tests with different positive and negative end feeding a forming limit curve can be constructed, dedicated to tubular hydroforming.

In the paper simulations are presented for the tests with different end feeding conditions, using shell elements. The influence of material parameters is investigated. Results of the FEM analysis are comparable with results from a Marciniak–Kuczynski analysis. Some salient differences can be attributed to the more realistic incorporation of boundary conditions in the FEM analysis. In the tensile/compression region, the M–K analysis requires a free displacement perpendicular to the main principal strain to have a neck developed at a specific angle to the loading direction. In a hydroforming test the lateral displacement of the sheet would result in a rotation along the tube axis, which is prevented by the seals. The constraint displacement results in a higher forming limit.

**Key words:** hydroforming, forming limit, yield locus, finite elements

## 1 INTRODUCTION

Tubular hydroforming is a relatively new and fast developing deformation technique. New tubular products, dedicated to hydroforming applications like press formed and laser welded Tubular Blanks, are currently entering the market. It is claimed that these products show improved formability behaviour for hydroforming applications compared to conventional roll formed and induction welded tubes. However, currently there is no standardized method to quantify the hydroformability of tubes. There is also a lack of knowledge about the actual tubular material properties. Most hydroforming processes are still analysed using sheet material properties, while it is known that the properties of the tubular material can differ significantly due to strain hardening introduced by the tube production process.

Free expansion testing with positive and negative axial feeding (pushing and pulling the tube ends) seems to be a promising technique to quantify the hy-

droformability of tubes [1]. Free expansion testing can be used to construct a total Forming Limit Curve (FLC) of tubes for the entire hydroforming process window. This will give vital design parameters for hydroforming applications of tubes.

This paper discusses the simulation of the free expansion test using a finite element code. The aim of the simulations is to investigate the applicability of the test for determination of hydroformability. The two main features of the simulations are the control of fluid flow and the determination of fracture.

## 2 THE FREE EXPANSION TEST

The purpose of a free expansion test is to expand a tube freely until failure occurs. This gives information about the failure behaviour of tubes under hydroforming conditions. Figure 1 illustrates the basic process steps of a typical free expansion test.

A free expansion test contains three stages. During

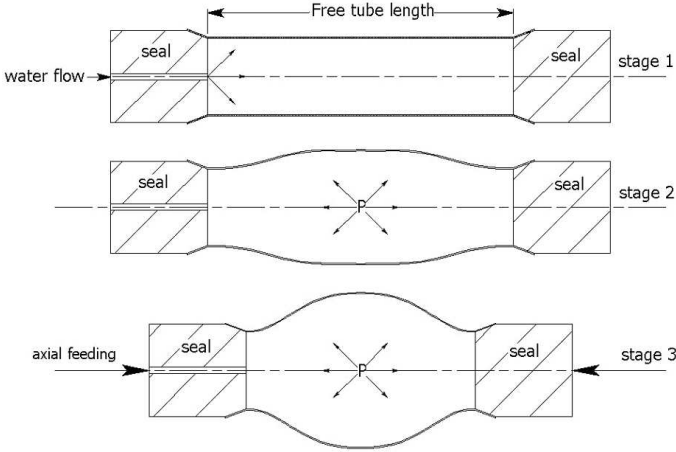


Figure 1: Free expansion test with axial feeding.

the first stage the tube is sealed. The tube ends are plastically deformed so the tube is fixed on the conical seals. Extra tools can be used to ensure the fixation on the seals. Then, the tube is filled through one of the seals with an emulsion of  $\pm 95\%$  water. In the second stage, the tube is pressurized resulting in a free expansion. Finally, in stage 3, feeding starts. This is achieved by pushing or pulling the seals (see Figure 1). The tube now expands further until failure occurs. The pressurization in stage 2 prevents the tube from early buckling and wrinkling. Currently, the free expansion test is mostly used as a qualitative test for tubes and the tests are performed without axial feeding. The radius after expansion is used as an indication of the tube quality. However, the test can also be used for the construction of an FLC for tubes. This FLC would enable the quantification of the hydroformability of tubes for different deformation states. An FLC is a common criterion used to predict failure for sheet forming processes. FLCs can be used if the through thickness stress is limited, and the deformation due to bending moments is limited [1]. Both conditions mentioned above are met by a free expansion test. Furthermore, an FLC depends on the strain path. Usually FLCs are presented for linear strain paths, but this is not strictly necessary and it will not be the case for the described loading sequence in the free expansion test.

To obtain deformations which are similar to the strain paths followed during the hydroforming process the strain path must be controlled during the test. Conventional free expansion rigs often apply pressure curves in combination with axial feeding, however this results in a very poor control over the strain path since there is no direct link between the applied pressure and the strain in the material. Control over the strain paths can be achieved by applying a volume flow in combination with axial feeding, this results in

a good control over the strain path, because the strains are a direct function of the volume change.

### 3 VOLUME CONTROLLED ANALYSIS

In a standard finite element program, the pressure and the displacements of the end of the tubes can easily be controlled as loads. However, in an experimental setup, the fluid flow and end-of-tube displacements are controlled. Usually, the pressure will first increase, reach a maximum and then decrease with a continuously increasing fluid volume. The decreasing pressure can not be modelled with a prescribed pressure load and is similar to the decreasing force in a buckling frame. In a structural analysis an arc-length method is used to overcome the maximum force (see e.g. [2]). Here, to overcome the maximum pressure, an arc-length type numerical control is developed that can be related to the inflow volume directly.

The volume change in a finite element analysis can easily be estimated from the equivalent force vector. Based on the equivalence of the work performed by the pressure and the equivalent force vector:

$$p dV = \mathbf{q}^T d\mathbf{u} \quad (1)$$

where  $p$  is the pressure,  $\mathbf{q}$  the corresponding equivalent force vector,  $V$  the volume and  $\mathbf{u}$  the nodal displacement vector. A first order approximation for a finite increment becomes:

$$p_{i,j} \Delta V_i = \mathbf{q}_{i,j}^T \Delta \mathbf{u}_{i,j} \quad (2)$$

where  $i$  denotes the increment number and  $j$  the iteration number of e.g. a Newton–Raphson process. A total increment of a quantity  $a$  is denoted by  $\Delta a$ , and an iterative change of that quantity by  $\delta a$ .

In a volume controlled analysis, the pressure  $p_{i,j}$  is not prescribed a priori, but will be adapted to the iteratively determined displacement increments in order to reach a prescribed volume increment  $\Delta V_i$ . A parameter  $\lambda$  is introduced to scale a unit pressure load  $\hat{p}$ :

$$p_{i,j} = \lambda_{i,j} \hat{p} \quad (3)$$

Correspondingly, a unit equivalent force vector  $\hat{\mathbf{q}}$  is defined such that

$$\mathbf{q}_{i,j} = \lambda_{i,j} \hat{\mathbf{q}}_{i,j} \quad (4)$$

Note that  $\hat{\mathbf{q}}$  is not a constant vector, but depends on the nodal displacements. The iterative displacement at iteration  $j$  is calculated from

$$\mathbf{K}_{i,j-1} \delta \mathbf{u}_{i,j} = \mathbf{r}_{i,j-1} + \delta \lambda_{i,j} \hat{\mathbf{q}}_{i,j-1} \quad (5)$$

where  $\delta\lambda_{i,j}$  is yet to be determined such that the volume constraint is fulfilled. The residue at the end of the previous iteration  $\mathbf{r}_{i,j-1}$  also takes account of the pressure  $p_{i,j-1}$ . A split solution strategy is used with

$$\delta\mathbf{a}_{i,j}^I = \mathbf{K}_{i,j-1}^{-1} \mathbf{r}_{i,j-1} \quad (6)$$

$$\delta\mathbf{a}_{i,j}^{II} = \mathbf{K}_{i,j-1}^{-1} \hat{\mathbf{q}}_{i,j-1} \quad (7)$$

leading to

$$\delta\mathbf{u}_{i,j} = \delta\mathbf{a}_{i,j}^I + \delta\lambda_{i,j} \delta\mathbf{a}_{i,j}^{II} \quad (8)$$

and

$$\Delta\mathbf{u}_{i,j} = \Delta\mathbf{u}_{i,j-1} + \delta\mathbf{a}_{i,j}^I + \delta\lambda_{i,j} \delta\mathbf{a}_{i,j}^{II} \quad (9)$$

Substituting (3), (4) and (9) into (2) leads to:

$$\lambda_{i,j} \hat{p} \Delta V_i =$$

$$\lambda_{i,j} \hat{\mathbf{q}}_{i,j}^T \left( \Delta\mathbf{u}_i^{i-1} + \delta\mathbf{a}_{i,j}^I + \delta\lambda_{i,j} \delta\mathbf{a}_{i,j}^{II} \right) \quad (10)$$

Because the unit equivalent force vector  $\hat{\mathbf{q}}_{i,j}$  depends on the yet unknown displacement, the last known vector  $\hat{\mathbf{q}}_{i,j-1}$  is used instead, resulting in the final equation for the iterative load increment:

$$\delta\lambda_{i,j} = \frac{\hat{p} \Delta V_i - \hat{\mathbf{q}}_{i,j-1}^T \left( \Delta\mathbf{u}_{i,j-1} + \delta\mathbf{a}_{i,j}^I \right)}{\hat{\mathbf{q}}_{i,j-1}^T \delta\mathbf{a}_{i,j}^{II}} \quad (11)$$

On convergence, the difference between  $\hat{\mathbf{q}}_{i,j}$  and  $\hat{\mathbf{q}}_{i,j-1}$  will vanish. Moreover, the constraint equation (2) already linearises the volume increment, ignoring the difference between  $\hat{\mathbf{q}}_{i-1}$  and  $\hat{\mathbf{q}}_i$  anyhow.

In Equation (2) the volume change due to the displacements of the loaded elements are taken into account. If axial feeding is used, this is represented in the model by a prescribed displacement on the end-nodes of the tube. The change in volume due to feeding ( $\Delta V_{\text{feed}} = A \Delta u_{\text{feed}}$ , with  $A$  the cross-section) and the prescribed fluid flow together define the  $\Delta V_i$  that must be applied in Equation (11). In the volume controlled analysis, the prescribed volume change per increment is adapted, based on the required number of iterations in the previous step.

The volume control was tested for a simple geometry, representing the rotation that is observed in free expansion tests with axial feeding. The error in the calculated volume change based on (2) was less than 1% when using 30 increments and of the order of 0.1% when using 100 increments. A complete tube expansion simulation is presented in Figure 2.

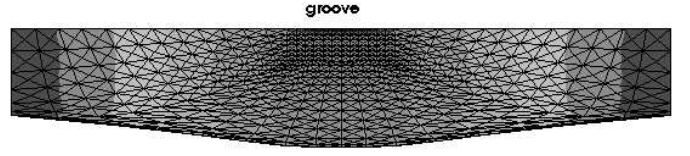


Figure 2: Volume controlled analysis of tube expansion.

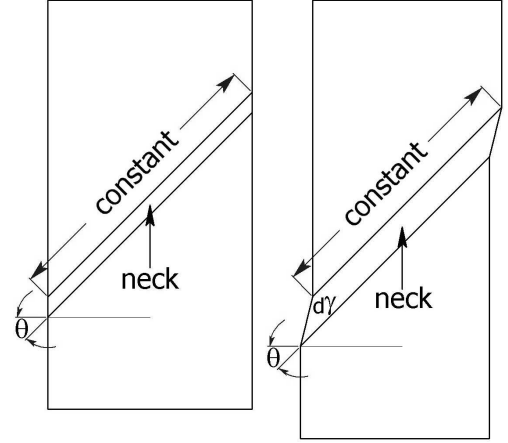


Figure 3: Sheet deformation according to the Hill criterion.

#### 4 PREDICTION OF FAILURE

The accurate prediction of failure is essential for the simulation of the free expansion test. Localized necking is—together with wrinkling—the most relevant failure mode in hydroforming of tubes. Two local necking criteria can be used without reference to the structure: the Hill localized necking criterion [3] and the Marciniak–Kuczynski (M–K) criterion [4]. For conventional stamping operations, the Hill criterion is used for the left-hand-side of the FLC (negative minor strain) and the M–K criterion is used for the right-hand-side (positive minor strain). The Hill criterion predicts a neck with an angle  $\theta$  with respect to the major strain direction (see Figure 3):

$$\cos 2\theta = -\frac{\varepsilon_1 + \varepsilon_2}{\varepsilon_2 - \varepsilon_1} \quad (12)$$

which represents a plane strain direction. If this angle is included in a M–K analysis, both criteria predict similar failure strains. For ordinary sheet forming simulations, a finite element simulation can mimic the M–K analysis [5]. The results depend mainly on the accuracy of the material model.

For a Nadai (Hollomon) hardening relation, the forming limit in the tensile–compression region is given by the straight line  $\varepsilon_1 + \varepsilon_2 = n$ . The angle of the neck, however, results in a lateral displacement as indicated in Figure 3. For a tube, this would result in a helical

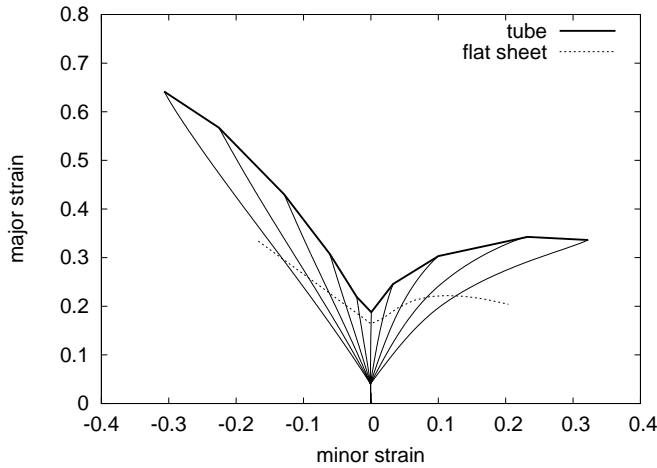


Figure 4: Hydroforming FLC.

localization and a rotation along the axis of the tube. This rotation is prevented by the seals and as a result fracture of a tube in hydroforming is always found coaxial with the tube axis. To initiate localization, a line of 13 nodes in the expected necking orientation is given a 2% lower thickness than the nominal thickness leading to an approximately 1% lower thickness in the connected elements (see Figure 2). The simulation was stopped when the strain rate in the neck was 10 times the strain rate in the uniform part of the model. The strain in the uniform part at that moment was used to create an FLC.

## 5 RESULTS

In Figure 4 the calculated FLC is presented together with an FLC, calculated with the M–K analysis for the same material, for a flat sheet. The constrained rotation clearly results in a steeper FLC in the compressive minor strain range. In the tensile minor strain range, it is clearly observed that the strain path is not linear and therefore a different FLC can be expected compared with ordinary (flat sheet) FLCs.

As with ordinary FLCs, the shape of the yield locus between the plane strain position and the equi-biaxial point strongly influences the right-hand-side of the FLC. An increase of the equi-biaxial stress with 2.5% will give a sharper yield locus than the original locus (Figure 5). The influence on the predicted FLC is given in Figure 6. This figure also shows that for a fixed fluid flow/axial feeding ratio, the reached strain ratio in the tensile–tensile region depends on the shape of the yield surface near the equi-biaxial point.

The calculations show the potential applicability of the free expansion test for hydroformability quantification. In future work, the calculations should be

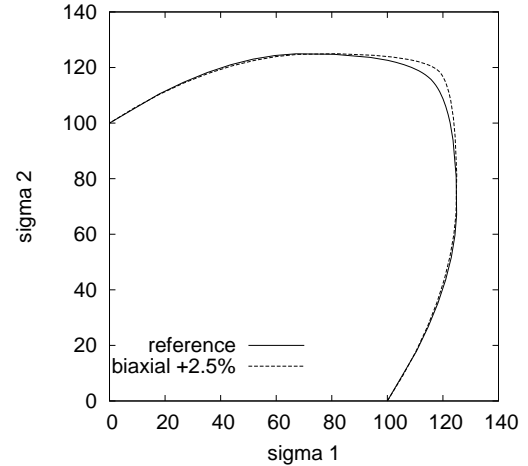


Figure 5: Yield locus with variation in equi-biaxial stress.

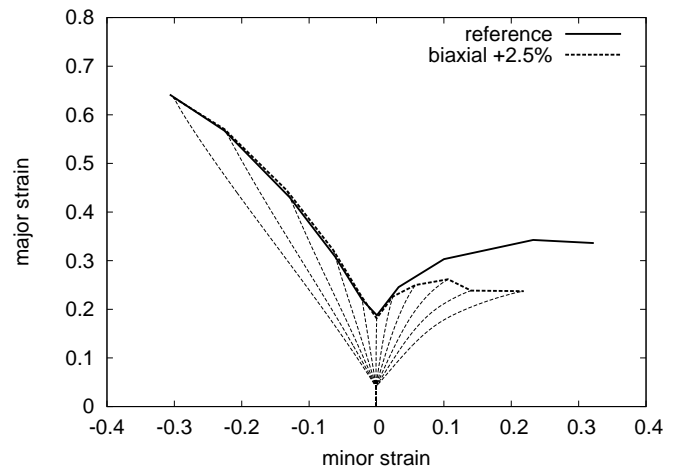


Figure 6: FLC with variation in equi-biaxial stress.

compared with actual experiments.

## REFERENCES

- [1] B. S. Levy. Recommendation on the forming limit curve for hydroforming steel. In *International Conference on Hydroforming*, pages 77–96, Germany, 1999.
- [2] M. A. Crisfield. *Non-linear Finite Element Analysis of Solids and Structures, volume 1: Essentials*. John Wiley & Sons, 1991.
- [3] R. Hill. On discontinuous plastic states, with special reference to localized necking in thin sheets. *Journal of the Mechanics and Physics of Solids*, 1:19–30, 1952.
- [4] Z. Marciniak and K. Kuczynski. Limit strains in processing of stretch forming sheet metal. *International Journal of Mechanical Sciences*, 9:609–620, 1967.
- [5] A. H. van den Boogaard and J. Huétink. Prediction of sheet necking with shell finite element models. In V. Brucato, editor, *The 6th International Esaform Conference on Material Forming*, pages 191–194, Salerno, 2003.